An acoustic and psychoacoustic assessment on the noise control of propellers in distributed propulsion configuration using phase-synchronisation

Session: Experimental Techniques

Bin Zang, University of Bristol, Bristol, United Kingdom,
nick.zang@bristol.ac.uk
Buda Turhan, University of Bristol, Bristol, United Kingdom,
en22804@bristol.ac.uk
Antonio J Torija, University of Salford, United Kingdom,
a.j.torijamartinez@salford.ac.uk
Carlos Ramos-Romero, University of Salford, United Kingdom,
c.a.ramosromero@salford.ac.uk
Mahdi Azarpeyvand, University of Bristol, Bristol, United Kingdom,
m.azarpeyvand@bristol.ac.uk

Abstract Distributed electric propulsion is widely recoginised as a promising propulsion configuration for next-generation aerial vehicles, including short-to-medium-haul passenger aircraft and urban air mobility vehicles. The presence of multiple propulsors gives rise to additional aerodynamic noise sources and yet, opportunities to novel noise control strategies. The present work examines the application of phase syncrhonisation technique to a DEP configuration, represented by two side-by-side propellers mounted to the leading-edge of a wing. Both the aeroacoustic and psychoacoustic analyses are performed on the far-field acoustic information. The results clearly show that when a relative phase difference is introduced between the two propellers, significant reduction of the tonal component at blade passing frequency can be achieved, accompanied by minor modifications to the directivity pattern. Moreover, such reduction leads directly to the reduction of loudness, a key indicator for the psychoacoustic annoyance. However, interestingly, the impulsiveness and sharpness indicators yield greater levels when the relative phase angle is increased. The findings from the work suggests that there could exist optimal phase angle for which the DEP configuration produces the least noise and psychoacoustic annoyance.

Keywords: Phase synchronisation, DEP psychoacoustics, Noise control

1. INTRODUCTION

Distributed electric propulsion (DEP) configuration is considered a promising candidate for next-generation aerial vehicles, from urban air mobility (Zhang et al., 2024) and to regional

short take-off and landing (Kim et al., 2018). The DEP design can potentially improve the aerodynamic performances as well as enabling better take-off and landing characteristics (Kim et al., 2018). Nevertheless, there exist several technological challenges when adopting propeller-driven configurations for these vehicles. Among which, the propulsive noise generated by the DEP configurations are recognised as the key barrier towards public acceptance and thus full implementation of the technology (S. A. Rizzi et al., 2020), since compared to the conventional turbofan engines, the DEP configuration is often open-rotor with limited noise shielding from a nacelle structure and moreover, the propulsor-airframe installation effects are significantly more pronounced (Chen et al., 2021).

The presence of multiple propellers in close proximity to each other as well as to the wing structure, regardless of the pusher or tractor configurations, mean that there are additional noise sources from propeller-propeller and propeller-wing interactions on top of the individual propeller. Pascioni and Rizzi (2018) investigated the tonal noise from a distributed propulsion unmanned aerial vehicle using the NASA noise prediction tool. They observed that for a pair of random phasing propellers, the tonal noise amplitude can differ up to 20 dB at a given observer location and more importantly, the directivity pattern was modified when compared to an isolated propeller. Their findings provide useful insights to the possible noise control strategies for a DEP configuration. Acevedo Giraldo et al. (2022) performed an analytical study on the tonal noise generated by a DEP configuration, which a pair of countrarotating propellers are mounted near the trailing edge of a wing. They concluded that comparing to the 'isolated' twin propellers (i.e., no installation effect from the wing), the tonal noise is significantly amplified due to the presence of the wing in vicinity of the propellers. By accounting for the blade-wing interaction and wing scattering effects, their analytical model was able to capture the tonal component satisfactorily. Turhan et al. (2023) performed an experimental investigation of the DEP configuration in forward flight over a range of incoming velocity from 8 m/s to 24 m/s at a fixed rotational speed of 8000 RPM (revolution-per-minute). From the coupled aerodynamic and aeroacoustic measurements, they reported that the thrust generated by the propellers were not influenced significantly by the separation distance between the two propellers, however, both the amplitude and directivity of the tonal noise at the blade passing frequency (BPF) and its harmonics varied notably with the separation.

Even though that the DEP configuration introduces additional installation effects, and thus, modifications to the noise characteristics, it also provides opportunities to noise control with the ability to fine-tune the operation of individual propeller (S. A. Rizzi et al., 2017). Pascioni et al. (2019) demonstrated that by carefully selecting the relative phase angle with respect to the blade position between two side-by-side propellers, an approximately 6dB noise reduction can be achieved at the BPF tone. Moreover, leveraging on the possible destructive interference between the two coherent noise sources, the directivity pattern can be modified, potentially steering the tonal component away from the pedestrian. Turhan et al. (2024) examined the effect of noise control on both the tonal and overall noise for a DEP configuration, where the phase angles of the pair of two-bladed propellers were varied from $0°$ (full synchronised) to $90°$ (maximum phase difference). They observed that the most significant noise reduction took place when the two propellers are fully out-of-sync (i.e., $90°$ apart). At the highest free-stream velocity of 24 m/s, it translated to 24 dB reduction for the BPF tone and 6 dB for the overall sound pressure level.

The amplitude of the noise, however, is often only one of the important indicators for psychoacoustic annoyance when it comes to perception of noise (Torija & Clark, 2021; Lotinga et al., 2023). Torija et al. (2022) examined the relationship between the first-order propeller parameters (e.g., propeller thrust, diameter) and the generation and perception of the propeller noise. Their psychoacoustic analysis from the listening test suggested that the tonality

and high-frequency contents, low-frequency modulation as well as the roughness and impulsiveness all contributed to the psychoacoustic annoyance from the propeller. Green et al. (2024) conducted a similar psychoacoustic study on an unmanned aerial aircraft, focusing on the different operational profiles, such as takeoff, landing, hovering and flyover. The results showed that the loudness was a principal factor for the psychoacoustic annoyance prediction. Furthermore, in the outdoor settings, the impulsiveness was closely associated with the psychoacoustic annoyance whereas in the indoor settings, tonality plays a more important role.

The results from the literature suggest that for a DEP configuration, despite the fact that a certain extent of noise reduction can be achieved by carefully controlling the relative phase angle between the propellers, it is not equivalent to mitigating the psychoacoustic annoyance from such a configuration. Moreover, studies relating the aeroacoustic and psychoacoustic characterisitics of a DEP configuration remain limited. Therefore, the present work reports on the noise signature from a small-scale DEP configuration when the relative phase angle of two propellers are maintained constant. Subsequently, psychoacoustic analysis, similar to those proposed in the previous studies, is undertaken to understand the impact of 'staggering' the relative phase angle on the actual perception of noise from the configuration. The work aims to provide some first-hand insights into the DEP noise so that further work can be carried out, possibly to investigate perception-driven control strategies. The remainder of this paper is organized as follows: a brief description of the experimental setup is presented in section 2. The results section (section 3) first discusses the noise characteristics of the DEP in subsection 3.1 and followed by the psychoacoustic analysis in subsection 3.2. Some concluding remark is provided in section 4, summarising this study's findings.

2. METHODOLOGY

2.1 Experimental Setup

The experiments were carried out in the aeroacoustic wind tunnel at the University of Bristol. The closed-circuit, open-jet wind tunnel has a jet nozzle exit dimension of 0.5 m (width) by 0.775 m (height). The nozzle is situated inside an anechoic chamber, which is fully anechoic down to 160 Hz (Mayer et al., 2019). Using this nozzle, the free-stream velocity ranges from 5 m/s to 40 m/s, with a turbulent intensity as low as 0.2%. The DEP set-up, securely mounted in the test chamber, is shown in Fig.1(a) and consists of two propellers and a NACA 0018 wing structure. The propellers are attached directly to the leading-edge of the wing in a side-by-side configuration, representative of the conventional DEP configuration (Kim et al., 2018; Pascioni & Rizzi, 2018).

Two identical 2-bladed propellers from Mejzlik were used so that a maximum phase difference of $90°$ can be achieved. Confined by the nozzle exit dimension, the propellers have a diameter of 228.6 mm (9 inch) and a fixed pitch-to-diameter (P/D) ratio of 1. They are driven by a pair of AT4125 T-motor brushless DC motor with a power rating of 2.2 kW. The wing structure, with a chord length of c = 300 mm and a span of L = 940 mm, was CNC-machined from aluminium. The distance between the propeller and the wing structure, accounting from the trailing-edge of the propeller to the leading-edge of the wing, was 150 mm, equivalent to approximately $0.66D$ separation. Moreover, from the previous work on the DEP configurations (Zarri et al., 2023; Turhan et al., 2023), it was shown that the blade-to-blade separation (s) had very limited impact on the aerodynamic performance of the propellers. Thus, to isolate the acoustic interference effects from the two propellers and avoid any potential aerodynamic interactions in the present set-up, the separation was fixed at $s = 0.05D$ (see Fig. 1(b) for the definition of the separation distance, s). The propeller-wing assembly was placed at a distance of 0.5 m away from the nozzle exit plane so that both propellers

were within the potential core region of the jet flow. Shao et al. (2022) revealed that phase synchronisation had more pronounced impact on the noise for a co-rotating multi-rotor system, therefore, the current set-up was also designed for the two propellers to co-rotate, in counter-clockwise sense of rotation when viewed from the front.
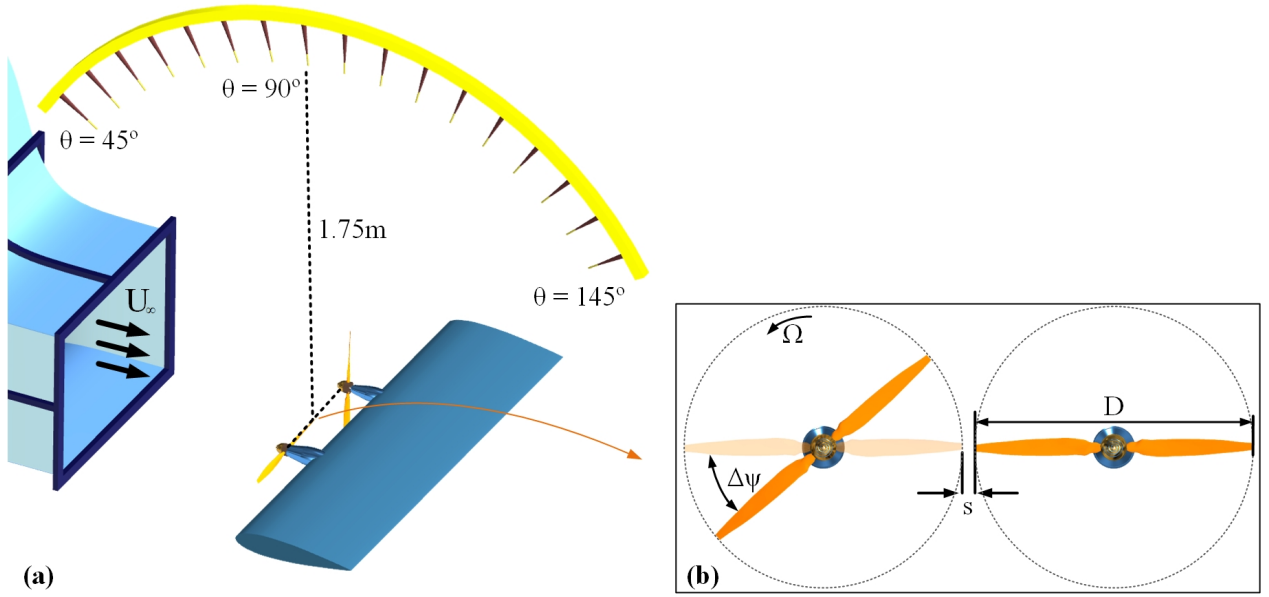
Figure 1: Schematic of the experimental setup in the wind tunnel. The top polar arc, oriented in the x-z plane, is shown, with the position of the upstream cylinder indicated.

To achieve accurate phase control, the angular position of the propeller has to be tracked at relatively high frequency. Thus, a 12-bit RE36IC incremental output encoder, with an uncertainty of $\pm 0.3\%$, was installed to each propeller. Signal from each of the encoder was simultaneously fed into the control loop and subsequently, the phase angles of both propeller were gradually adjusted with a minor correction until the required relative phase angle was obtained. Here, the relative phase angle, $\Delta\psi$, was defined as the angle between the angular position of the two propellers, as shown in Fig. 1(b). If one of the propeller was designated the 'master' propeller, then the other would be trailing the master propeller by an angle of $\Delta\Psi$ (thus, the sign convention for $\Delta\psi$ is neglected). An earlier study performed using the same set-up showed that when the same relative phase angle was set and repeated, the variations of the noise level were within 2 dB, confirming the validity of feedback control strategy implemented on the present set-up (Turhan et al., 2023). In this study, four distinct relative phase angles of $\Delta\psi = 0°$, 60°, 75° and 90° were chosen to help understand the acoustic and psychoacoustic effects on the phase-syncrhonised DEP.

An array of far-field microphones, shown in Fig. 1(a), were used to collect acoustic information from the DEP configuration, capturing both the amplitude and directivity. The array consists of 21 free-field GRAS 40PL microphones, covering a range of observer angles from 45° to 145° at 5° interval. Furthermore, the array was perpendicular to the wing and aligned with the centre between the two propellers, representative of the pedestrian orientation. Data from all the microphones were simultaneously recorded using National Instruments PXI4499 sound and vibration module, at a sampling rate of 2^{16} Hz and a sampling duration of 16 s. To calculate the power of acoustic pressure in frequency domain, the data were then Fourier transformed using Welch's method. The power spectral density (PSD) of the acoustic pressure is determined as: $\text{PSD}(f) = 10 log_{10}(\phi_{pp}(f)/p_0^2)$, where $\phi_{pp}(f)$ is the frequency-domain acoustic pressure power and $p_0 = 20 \times 10^{-6}$ Pa is the reference pressure. To obtain the amplitude of the BPF tone, the PSD is integrated around the BPF over a range of 164 Hz $\leq f \leq$

172 Hz as: $\text{SPL}_{\text{BPF}} = 10 log_{10}(\int \phi_{pp}(f) \cdot df / p_0^2)$.

2.2 Psychoacoustic Analysis

When considering and predicting the human hearing perception of the aerial vehicles, psychoacoustic metrics are considered to perform better than the conventional noise metrics, such as EPNL (S. Rizzi, 2016; Torija et al., 2019). In recent studies, these metrics have been widely adopted to model psychoacoustic annoyance associated with rotors (Torija & Clark, 2021) , rotorcrafts (Boucher et al., 2023) and unmanned aerial vehicles (Green et al., 2024).

There are several sound quality metrics (SQMs) which are essential to the evaluation of psychoacoustic annoyance, namely, Loudness (N), Sharpness (S), Fluctuation Strength (FS), Roughness(R), Tonality (T) and Impulsiveness (I). Loudness, measured in sone, provides a measurement of the perceptual sound intensity. In this paper, the impulsiveness is calculated using the ECMA-418-2 overall binaural model (Ecma International, 2022). Sharpness, in acum, specifically describes the perception of the sound imbalance towards high-frequency region, and is calculated based on ISO 532-3 loudness model (ISO Acoustics Technical Committee, 2023) with Aures weighting. Fluctuation Strength, in vacil, measures the perception of slower modulations occurring at very low frequencies, up to about 20 Hz, with a peak around 4 Hz, and is also calculated using the ECMA-418-2 overall binaural model. In contrast, Roughness, in asper, (R) measures the perception of rapid sound modulation within the frequency range between 15 and 300 Hz, with a peak around 70 Hz.Tonality, measured in tonality units TU, gives a more direct evaluation of the prominence of the discrete tones. Both Tonality and Roughness are caculated according to Sottek's hearing model (Sottek, 1993). Lastly, Impulsiveness, measured in impulsiveness units IU, focuses on determining the perception of short, sudden changes in sound; and has been calculated using the Sottek's hearing model.

Torija et al. (2022) carried out an extensive experimental campaign on rotor noise with a hearing tests using the scaled noise signature from the measurements. Based on the empirical results, they proposed an improved psychoacoustic annoyance (PA) model, taking into account of the aforementioned SQMs:

$$PA = N_5(1 + \sqrt{\gamma_0 + \gamma_1 w_S^2 + \gamma_2 w_{FR}^2 + \gamma_3 w_T^2 + \gamma_4 w_I^2}), \tag{1}$$

where N_5 is the 5th percentile of the Loudness metric. w_S^2 is the sharpness factor and w_{FR}^2 is the integrated factor of fluctuation strength and roughness developed by Zwicker and Fastl (2013). Moreover, w_T^2 and w_I^2 denote the tonality (More, 2010) and impulsiveness factors, respectively. Here, the impulsiveness factor is defined as $w_I^2 = \frac{0.075 \cdot I}{N^{-1.334}}$. The five γ coefficients are calculated using a non-linear regression: $\gamma_0 = 103.08$, $\gamma_1 = 339.49$, $\gamma_2 = 121.88$, $\gamma_3 = 77.20$ and $\gamma_4 = 29.29$. It is worthwhile to mention that the 5th percentile values are utilised to compute all the input factors to the PA model (Torija et al., 2022).

3. RESULTS AND DISCUSSION

3.1 Far-field acoustics of the DEP configuration

For a propeller in forward flight with a free-stream velocity, U_∞, it is conventional to define the the advance ratio, J:

$$J = \frac{U_\infty}{nD}, \tag{2}$$

where n denotes the number of revolution per second and D is the propeller diameter. For the present test cases, the rotational speed (Ω) of the propeller is kept at 5000 RPM. Therefore, at the given $n = \Omega/60 \approx 83.33$ and $D = 228.6$ mm, two free-stream velocities were investigated to examine the effect of advance ratio on the DEP noise at $U_\infty = 9$ m/s and 14 m/s, corresponding to $J = 0.47$ and 0.73, respectively.
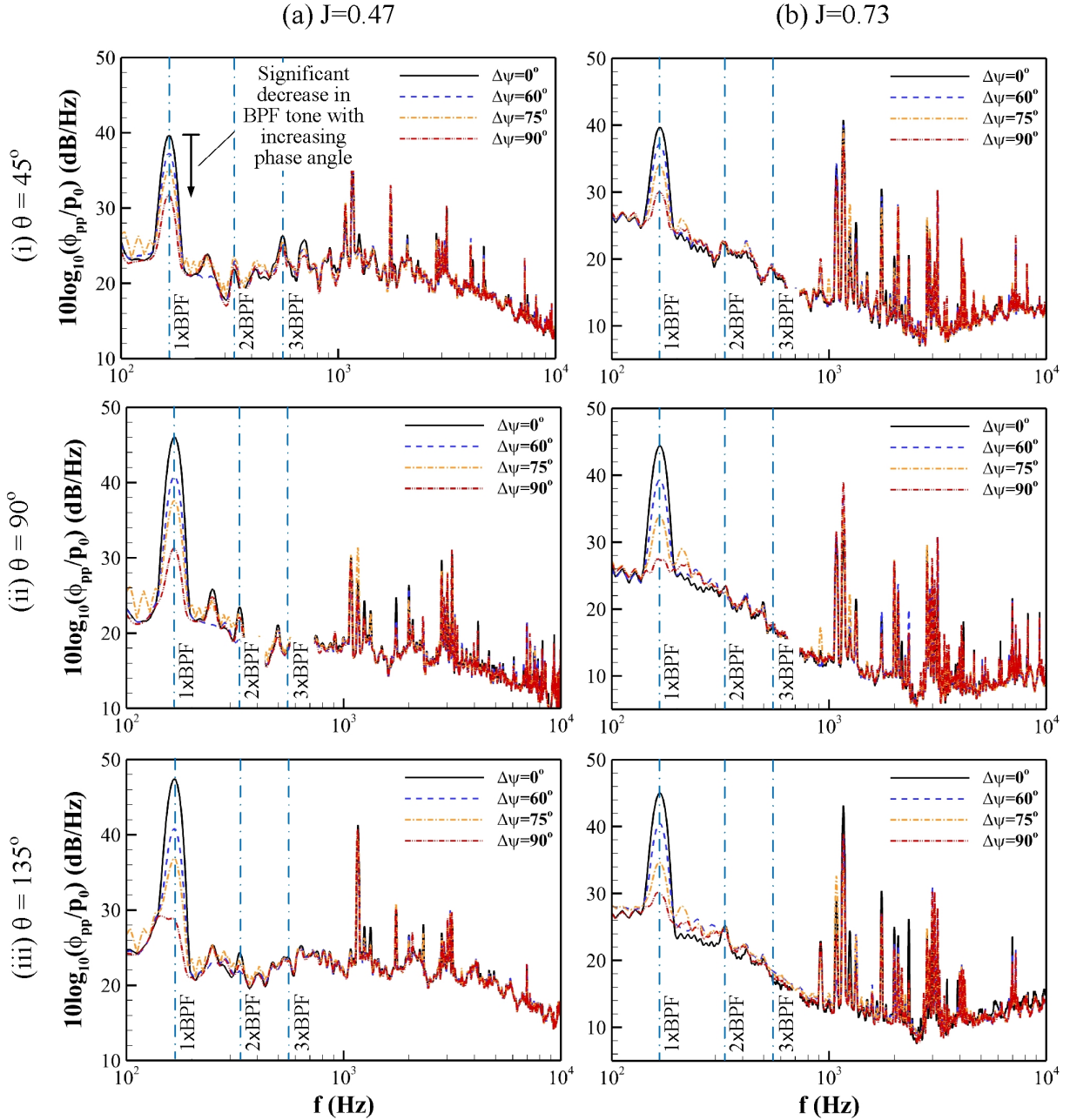
Figure 2: Far-field acoustic spectra of the phase-synchronised DEP configuration ($\Delta\psi = 0°$, $60°$, $75°$, $90°$) at two different advance ratios of (a) $J = 0.47$ and (b) $J = 0.73$ at three observer angles of $\theta = 45°$ (upstream), $90°$ (directly below) and $135°$ (downstream).

Figure 2 first show the far-field acoustic pressure spectra at the two advance ratios of $J = 0.47$ and 0.73 when the two propellers are phase-synchronised with relative phase angle differences of $\Delta\psi = 0°$, $60°$, $75°$, $90°$. Recall that for the two-bladed propellers used in the study, $\Delta\psi = 0°$ means that the two propellers are fully in-phase and conversely, $\Delta\psi = 90°$ fully out-of-phase. The observer angles selected are $\theta = 45°$, $90°$ and $135°$, which correspond to upstream, directly below and downstream of the propeller plane of rotation, with respect to the free-stream direction. At first glance, the acoustic spectra are characterised by

the presence of multiple tones, most prominent at the fundamental blade passing frequency of $f = \Omega \cdot n_{blade} \approx 166.67$ Hz (note that N_{blade} is the number of blades for the propeller, as well as some extent of broadband contents at mid-to-high frequencies (e.g., 1000 Hz $\leq f \leq$ 5000 Hz). The latter is more pronounced at the lower advance ratio. These characteristics are typical for the aerodynamic noise generated by propellers and agree well with the literature (Greenwood et al., 2022). A closer examination reveals that varying the relative phase angle between the two propellers have significant impact on the tonal amplitude of the BPF, regardless of the advance ratio and observer angle. In particular, when relative phase angle increases from $\Delta\psi = 0°$ to $90°$, the reduction in BPF tone exceeds 10 dB, indicating that phase synchronisation is highly effective in mitigating the fundamental tonal component, consistent with the previous findings (Pascioni et al., 2019).

Comparing across the different observer locations (see Figs. 2(a)(i) to (a)(iii)), the highest reduction in the BPF tone occurs at downstream observer angle of $\theta = 135°$, suggesting that introducing a relative phase angle to the two propellers not only reduces the amplitude of the BPF tone, but also modifies the directivity. This will be examined in more detail in the following discussion. Moreover, the effect of advance ratio can also be discerned, as shown in Figs. 2(a) and (b). At the higher advance ratio, the extent of reduction in the BPF tone appears to be less influenced by the observer angle than that of the lower advance ratio. Consequently, the magnitude associated with the reduction is comparable to the lower advance ratio at upstream locations, but falls short at the other observer locations. It is also interesting to note that increasing the relative phase angle between the propellers shows limited impact on the higher harmonics of the BPF as well as the broadband component, corroborating to the fact that the mitigation is mainly attributed to the acoustic destructive interference between the two coherent sound sources in close promixity (Pascioni et al., 2019; Shao et al., 2022).

It is clear from the acoustic spectra that phase synchronisation mainly acts on the fundamental BPF tone. Hence, the directivity pattern of the BPF tone is investigated instead of the conventional overall sound pressure level. Figure 3 shows the directivity pattern for the two advance ratios and four distinct relative phase angles, similar to that of the acoustic spectra. In general, the directivity of the BPF tone exhibits a cardioid pattern with noticeable amplifications towards the downstream direction. Yet, the most notable changes can be observed when the directivity from $\Delta\psi = 0°$ and $90°$ are compared. At lower advance ratio of $J = 0.47$, the greater attenuation at the downstream observer angles for the fully out-of-sync case ($\Delta\psi = 90°$) gives rise to more 'downstream-tilted'. At higher advance ratio of $J = 0.73$, a stronger reduction of BPF is observed in the plane of rotation when the propellers become increasingly out-of-sync, which as will be shown in the psychoacoustic analyses later to result in lower loudness at $\theta = 90°$.
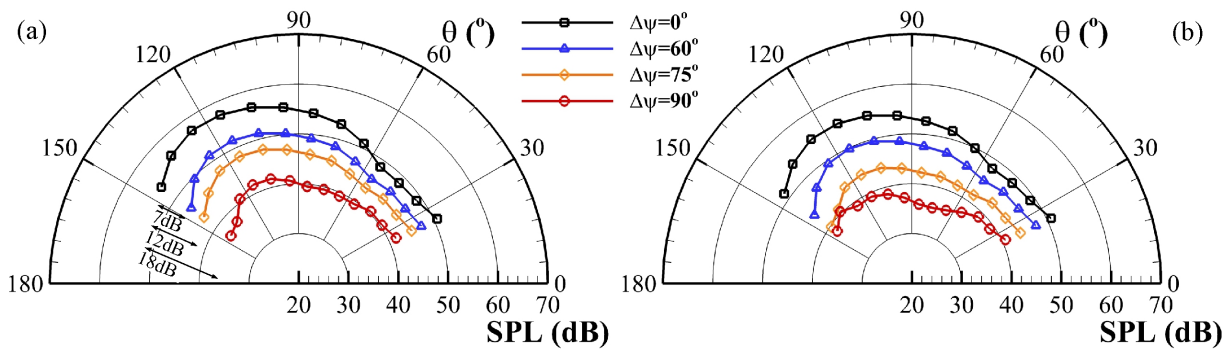
Figure 3: Directivity of the integrated BPF tone ($\mathrm{SPL_{BPF}}$) for the phase-synchronised DEP configuration ($\Delta\psi = 0°, 60°, 75°, 90°$) at two different advance ratios of (a) $J = 0.47$ and (b) $J = 0.73$, respectively.

Considering the fact that perception of the DEP noise is likely to be directly related to

not only the amplitude (e.g., loudness) of the noise itself, but also its temporal domain and frequency content (e.g., impulsiveness and sharpness), it is useful to examine and understand the temporal evolution of the DEP noise at different relative phase angles. To obtain the temporal information on the far-field acoustic pressure, a wavelet transform (Turhan et al., 2024) has been performed and the contour map of its coefficient magnitude is shown in Fig. 4, illustrating the temporal features of the acoustic pressure at a given frequency. The BPF tone at approximately $f = 166.67$ Hz reveal drastically different behaviour when the relative phase angle, $\Delta\psi$, is increased. At $\Delta\psi$ 0°, the tone has a relatively consistent presence over time, signifying a 'almost' constant-amplitude emission of the BPF tone. As the relative phase angle is increased to 60° 75° and 90°, such coherence in the BPF tone gradually disappears, and instead, the emission of the BPF tone becomes more impulsive, indicated by the short burst of energy over time. The changes in the temporal characteristics of the BPF tone will impact on the perception of this tonal noise, which will be further explored using the psychoacoustic indicators in the next section.
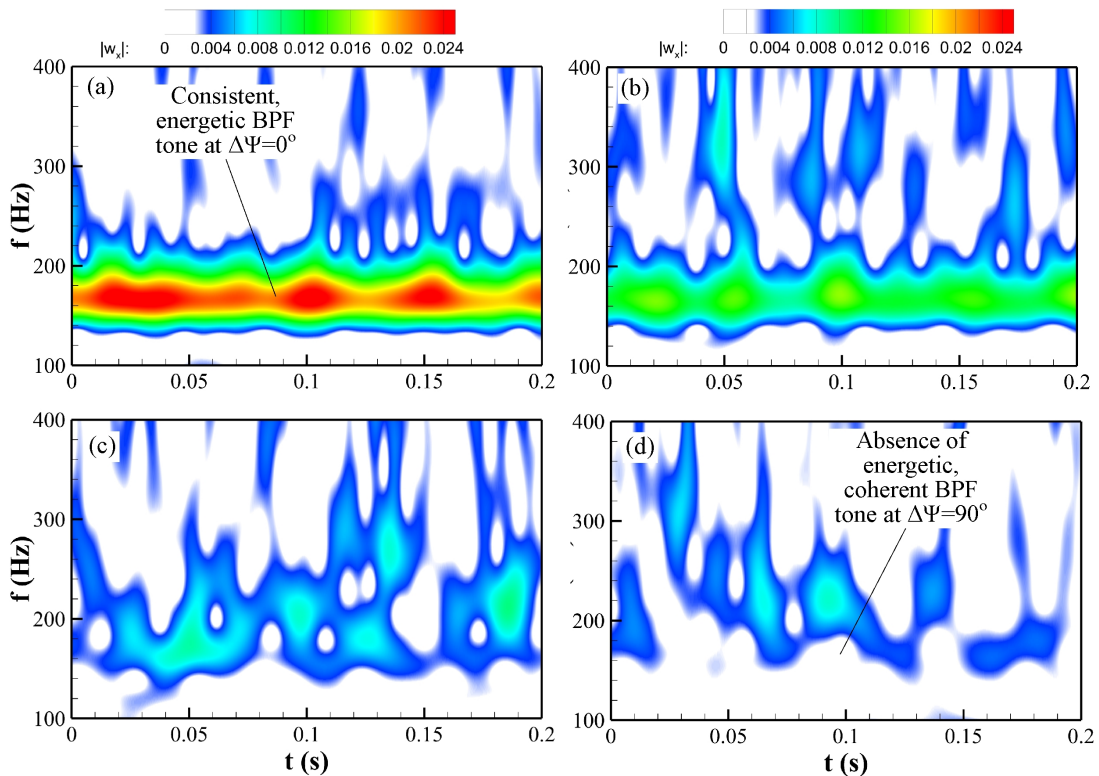
Figure 4: Contour map of the wavelet coefficient magnitude, $|w_x|$, showing the temporal evolution of the acoustic pressure for (a) $\Delta\psi = 0°$, (b) $\Delta\psi = 60°$, (c) $\Delta\psi = 75°$ and (d) $\Delta\psi = 90°$.

3.2 Psychoacoustic analysis of the phase-synchronised propellers

As suggested by Torija et al. (2022), it is important to include several indicator related with sound quality and perception, such as loudness, sharpness, tonality and impulsiveness, to better understand and predict the psychoacoustic annoyance from a propeller. Therefore, the far-field acoustic signals were passed through each of these analyses and the results are shown in Fig. 5. The same three observer angles as the acoustic spectra results, namely $\theta = 45°$, 90° and 135°, are chosen to keep the analysis consistent. Both advance ratios are included in the same figure, and differentiated by either 'filled' ($J = 0.47$) or 'empty' ($J = 0.73$) symbol. As expected, at a given advance ratio, the fully synchronised propellers are the loudest (see Fig 5(a)), and moreover, when operating at the lower advance ratio, the two propellers with relative phase of $\Delta\psi = 90°$ can become even louder than that of $\Delta\psi = 0°$ at higher advance ratio and both upstream and downstream observer angles. This can possibly

be attributed to the heightened broadband component at the lower advance ratio. Moreover, tonality exhibits higher amplitudes at higher advance ratios, which correlates with the results presented in Fig. 2. Although the amplitude of the BPF is higher at $J = 0.47$, other frequency interactions are also present, such as peaks at the $2{\times}$BPF and $3{\times}$BPF harmonics, which could penalize the tonality. The higher tonality at $J = 0.73$, particularly visible at $\theta = 90°$ is because firstly that the tonal noise at $1\text{kHz} \leq f \leq 4\text{kHz}$ are clearly higher compared to the case with lower advance ratio and secondly, the tonal amplitude at the BPF tends to be the most prominent for $f \leq 1\text{kHz}$ with significantly lower amplitudes of the harmonics. More interestingly, when the sharpness (Fig. 5(b)) and impulsiveness (Fig. 5(d)) indicators are evaluated, the trend is reversed: the $\Delta\psi = 90°$ case exhibits the highest sharpness and impulsiveness, at all three observer angles examined. The earlier observation from the temporal evolution of the far-field acoustics reveals that increasing the relative phase angle could potentially lead to shorter 'burst' of energy at the BPF tone, which partly explains the accentuating sharpness and impulsiveness seen with the increasing relative phase angle. Nevertheless, similar to loudness, the lower advance ratio case is consistently higher than the higher advance ratio counterpart for these two indicators.
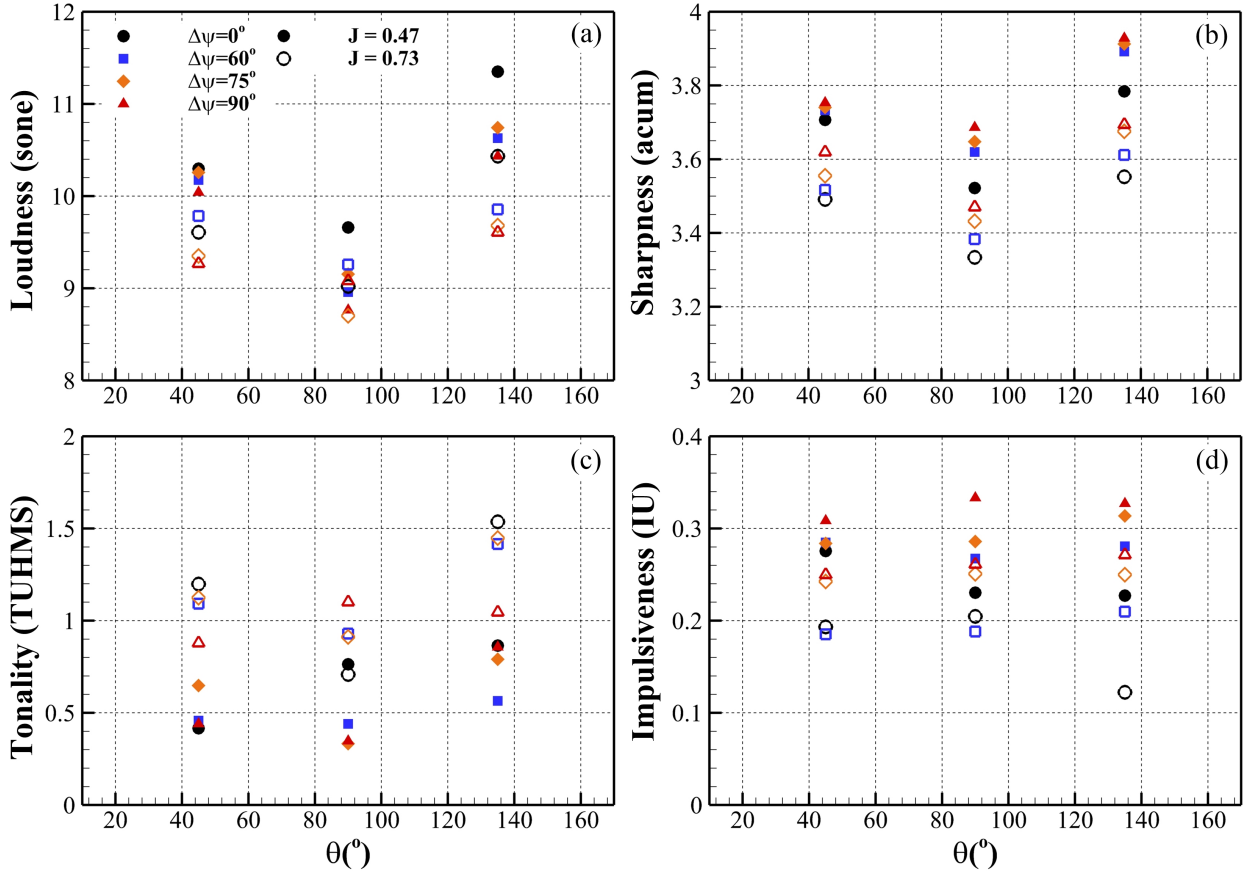
Figure 5: Psychoacoustic indicators of (a) Loudness (ECMA-418-2 overall binaural model, (Ecma International, 2022)), (b) Sharpness (ISO 532-2 model, (ISO Acoustics Technical Committee, 2023)) with Aures weighting, (c) Tonality (Sottek's hearing model, (Sottek, 1993)) and (d) Impulsiveness (Sottek's hearing model, (Sottek, 1993)) analysed from the far-field acoustic signal for the DEP configurations at the two advance ratios ($J = 0.47$ and 0.73) and four relative phase angles ($\Delta\psi = 0°$, $60°$, $75°$ and $90°$).

The psychoacoustic annoyance of the recorded far-field noise from the DEP is subsequently evaluated, taking into account of all the indicators mentioned above (Torija et al., 2022; Lotinga et al., 2023), and the results are shown in Fig. 6. Observing the results, there are three key features that are worth highlighting. Firstly, increasing the advance ratio helps reduce the psychoacoustic annoyance level. Assuming that at any instance of the flight, the

free-stream velocity remains roughly constant and the diameter of the propeller is fixed, the psychoacoustic annoyance can thus be mitigated by reducing the rotational speed of the propeller. Secondly, modifying the relative phase angle from $\Delta\psi = 0°$ to $90°$ indeed reduces the annoyance, reaffirming that phase synchronisation is a viable revenue for noise control. Thirdly, comparing the psychoacoustic annoyance levels across the observer angles, it is clear that for a specific advance ratio, the upstream and downstream locations have higher levels of psychoacoustic annoyance compared to the locaton directly underneath the propellers.
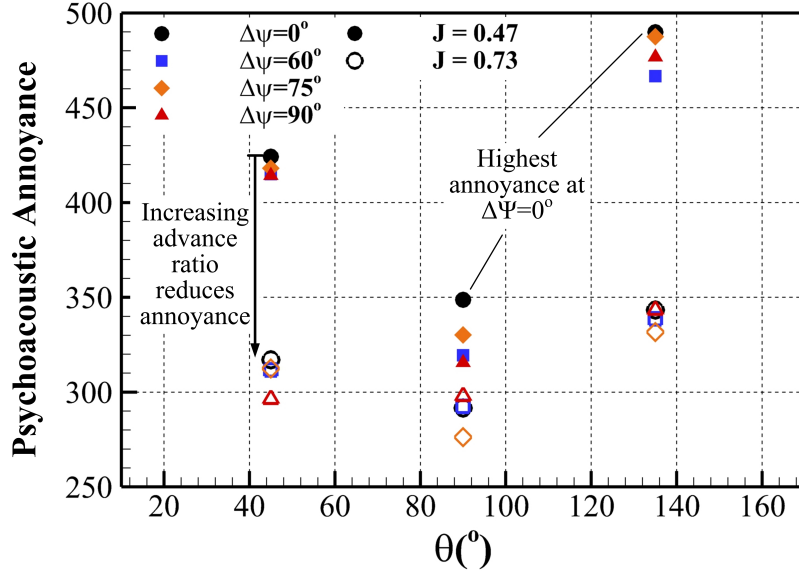
Figure 6: Psychoacoustic annoyance from the DEP noise, taking into account of the contribution from all the SQMs for the two advance ratios ($J = 0.47$ and 0.73) and four relative phase angles ($\Delta\psi = 0°$, $60°$, $75°$ and $90°$). The annoyance is calculated based on the psychoacoustic model in (Torija et al., 2022).

4. CONCLUSION

An experimental campaign has been undertaken to examine the aeroacoustic and psychoacoustic characteristics of a DEP configuration in forward flight. Particular interest is focused on exploring the noise control strategy by adjusting the relative phase angle between the propellers, i.e., phase synchronisation technique. The experimental set-up consists of two side-by-side propellers operating in forward flight condition at two advance ratios of 0.47 and 0.73. The relative phase between the two propellers are carefully adjusted to four distinct angles of 0°, 60°, 75° and 90°. The far-field acoustic results show that increasing the relative phase angle from fully in-phase to fully out-of-phase significantly reduces the BPF tone, regardless of the observer angles and advance ratios. Nevertheless, it also leads to a loss of coherence in the emission of the tonal component in temporal domain. When psychoacoustic analysis is applied to the recorded acoustic signal, the four indicators, loudness, tonality, sharpness and impulsiveness behave differently. Despite the fact that the 0° relative phase angle case dominates the loudness, both the sharpness and impulsiveness see a reversed trend, which the 90° relative phase angle case gives rise to higher levels. Finally, the psychoacoustic annoyance of the DEP configuration is evaluated and clearly illustrates that increasing the advance ratio during a given stage of the flight and introducing a relative phase angle between the two propellers can lead to amelioration of the psychoacoustic annoyance, and indeed, phase synchronisation is a potentially viable noise control strategy. Further studies on its impact to the higher harmonics and broadband components are needed to fully optimise such strategy.

5. REFERENCES

Acevedo Giraldo, D., Roger, M., Jacob, M. C., & Beriot, H. (2022). Analytical study of the aerodynamic noise emitted by distributed electric propulsion systems. In *28th aiaa/ceas aeroacoustics 2022 conference* (p. 2022-2830).

Boucher, M. A., Krishnamurthy, S., Christian, A. W., & Rizzi, S. A. (2023). Sound quality metric indicators of rotorcraft noise annoyance using multilevel analysis. *The Journal of the Acoustical Society of America*, *153*(2), 867–876.

Chen, B., Yakovlev, A., & Moshkov, P. (2021). Fast prediction method of aircraft noise with distributed propulsion in the far field. In *Journal of physics: Conference series* (Vol. 1925, p. 012007).

Ecma International. (2022). *Ecma-418-2:2022 psychoacoustic metrics for itt equipment — part 2 (models based on human perception)* (Vol. ECMA Tech. Report; Tech. Rep.).

Green, N., Torija, A. J., & Ramos-Romero, C. (2024). Perception of noise from unmanned aircraft systems: Efficacy of metrics for indoor and outdoor listener positions. *The Journal of the Acoustical Society of America*, *155*(2), 915–929.

Greenwood, E., Brentner, K. S., Rau, R. F., & Ted Gan, Z. F. (2022). Challenges and opportunities for low noise electric aircraft. *International Journal of Aeroacoustics*, *21*(5-7), 315–381.

ISO Acoustics Technical Committee. (2023). *Iso532-3: 2023 acoustics — methods for calculating loudness — part 3: Moore-glasberg-schlittenlacher* (Vol. Tech. Report; Tech. Rep.). International Organization for Standardization.

Kim, H. D., Perry, A. T., & Ansell, P. J. (2018). A review of distributed electric propulsion concepts for air vehicle technology. In *2018 aiaa/ieee electric aircraft technologies symposium (eats)* (pp. 1–21).

Lotinga, M. J., Ramos-Romero, C., Green, N., & Torija, A. J. (2023). Noise from unconventional aircraft: a review of current measurement techniques, psychoacoustics, metrics and regulation. *Current Pollution Reports*, *9*(4), 724–745.

Mayer, Y. D., Jawahar, H. K., Szőke, M., Showkat Ali, S. A., & Azarpeyvand, M. (2019). Design and performance of an aeroacoustic wind tunnel facility at the university of bristol. *Applied Acoustics*, *155*, 358–370.

More, S. R. (2010). *Aircraft noise characteristics and metrics* (Unpublished doctoral dissertation). Purdue University, United States.

Pascioni, K. A., & Rizzi, S. A. (2018). Tonal noise prediction of a distributed propulsion unmanned aerial vehicle. In *2018 aiaa/ceas aeroacoustics conference* (p. 2018-2951).

Pascioni, K. A., Rizzi, S. A., & Schiller, N. (2019). Noise reduction potential of phase control for distributed propulsion vehicles. In *Aiaa scitech 2019 forum* (p. 2019-1069).

Rizzi, S. (2016). Toward reduced aircraft community noise impact via a perception-influenced design approach. In *Inter-noise congress and conference proceedings* (Vol. 253, pp. 220–244).

Rizzi, S. A., Huff, D. L., Boyd, D. D., Bent, P., Henderson, B. S., Pascioni, K. A., . . . others (2020). *Urban air mobility noise: Current practice, gaps, and recommendations* (Tech. Rep.). (No. NASA/TP-20205007433)

Rizzi, S. A., Palumbo, D. L., Rathsam, J., Christian, A. W., & Rafaelof, M. (2017). Annoyance to noise produced by a distributed electric propulsion high-lift system. In *23rd aiaa/ceas aeroacoustics conference* (p. 2017-4050).

Shao, M., Lu, Y., Xu, X., Guan, S., & Lu, J. (2022). Experimental study on noise reduction of multi-rotor by phase synchronization. *Journal of Sound and Vibration*, *539*, 117199.

Sottek, R. (1993). *Modelle zur signalverarbeitung im menschlichen gehör* (Unpublished doctoral dissertation). RWTH Aachen, Germany. ("Models for signal processing in human hearing")

Torija, A. J., & Clark, C. (2021). A psychoacoustic approach to building knowledge about human response to noise of unmanned aerial vehicles. *International Journal of Environmental Research and Public Health*, *18*(2), 682.

Torija, A. J., Li, Z., & Chaitanya, P. (2022). Psychoacoustic modelling of rotor noise. *The Journal of the Acoustical Society of America*, *151*(3), 1804–1815.

Torija, A. J., Roberts, S., Woodward, R., Flindell, I. H., McKenzie, A. R., & Self, R. H. (2019). On the assessment of subjective response to tonal content of contemporary aircraft noise. *Applied Acoustics*, *146*, 190–203.

Turhan, B., Jawahar, H. K., Gautam, A., Syed, S., Vakil, G., Rezgui, D., & Azarpeyvand, M. (2024). Acoustic characteristics of phase-synchronized adjacent propellers. *The Journal of the Acoustical Society of America*, *155*(5), 3242–3253.

Turhan, B., Kamliya Jawahar, H., Bowen, L., Rezgui, D., & Azarpeyvand, M. (2023). Aeroacoustic characteristics of distributed electric propulsion system in forward flight. In *Aiaa aviation 2023 forum* (p. 2023-4490).

Zarri, A., Koutsoukos, A., & Avallone, F. (2023). Aerodynamic and acoustic interaction effects of adjacent propellers in forward flight. In *Aiaa aviation 2023 forum* (p. 2013-4489).

Zhang, J., Liu, Y., & Zheng, Y. (2024). Overall evtol aircraft design for urban air mobility. *Green Energy and Intelligent Transportation*, *3*(2), 100150.

Zwicker, E., & Fastl, H. (2013). *Psychoacoustics: Facts and models* (Vol. 22). Springer Science & Business Media.